

Chapter Five : Conclusion and Discussion

Mobile phones have monopole antennas that give rise to omni directional radiation patterns in the plane perpendicular to the monopole. Due to this omni directional property of the radiation pattern, signals are emitted from antennas in all directions. It is possible that some of the signals could enter the brain of the user as well. Energy in the signals that enter the brain can cause heating and therefore damage the brain cells. This is a problem for concern.

Using Specific Absorption Rate (SAR) it was easy to understand the rate of heating. Assuming the brain to be divided into 1000 cubic cells, calculations of SAR values were carried out for three cases of brain alone; for the brain and skull together; and for the brain, skull and the ears all together. The SAR values seem to be higher at middle than at the periphery of the brain and the maximum value of the SAR is below the safety standards set by British safety levels.



University of Moratuwa, Sri Lanka.
Electronic Theses & Dissertations
www.lib.mrt.ac.lk

Even then, since some people are using these instruments for long periods of time, and since children are using them it is better to minimize the SAR as far as possible.

To minimize such absorption an attempt was made to design a suitable antenna for the mobile unit, which would reduce the electromagnetic waves propagation to the head of a user.

The general trend of miniaturization, microstrip patch antennas on small size substrates give rise to many practical applications. In mobile communication systems, the antenna size has often to be reduced as far as possible. For convenience I selected microstrip antenna because of its small size and due to its low cost.

There are two types of antennas in use, rectangular and circular. For easy calculations a rectangular shape was selected for the antenna design.

Initially phase difference (δ) and distance between two patches (d) were kept constant but number of patches were varied. In this regard a single patch antenna, a two-patch array and a four patch linear array were considered. The most appropriate broad beam is given by two patches antenna.

Then the two elements square-patch microstrip antenna was designed, fabricated and tested and the phase difference (δ) and the distance between two patches (d) were varied. The antenna showed a broad beam with empty radiation regions when the two elements were separated by a $\lambda/2$ (λ is the wave length) and when the two elements were fed by units of equal magnitude by $\pi/2$. We applied shielding effect for selected antenna. Then the radiation pattern is broader than the earlier one and there was a region which receives less amount of back radiations or no radiations passing through this area. This area is more suitable to keep our head. This method reduces the electromagnetic radiation absorbed by the brain.



Normally the frequency of the signal is in the range of (824-900) MHz. But using the material with permitivity as 2.91, it is difficult to make an antenna for the cellular phones, because the dimension of the antenna is too large. Then it is possible to design an antenna for the frequency of 9.4GHz to demonstrate the principle.

The effective design of components related to the mobile phones mounted on hand held units should have the following requirements,

It should be small and flat, low cost, attractive in appearance, easy to construct and thus following shape of the radiation pattern is recommended.

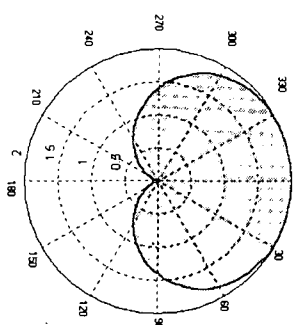


Figure 5.1: Required radiation pattern for the antenna

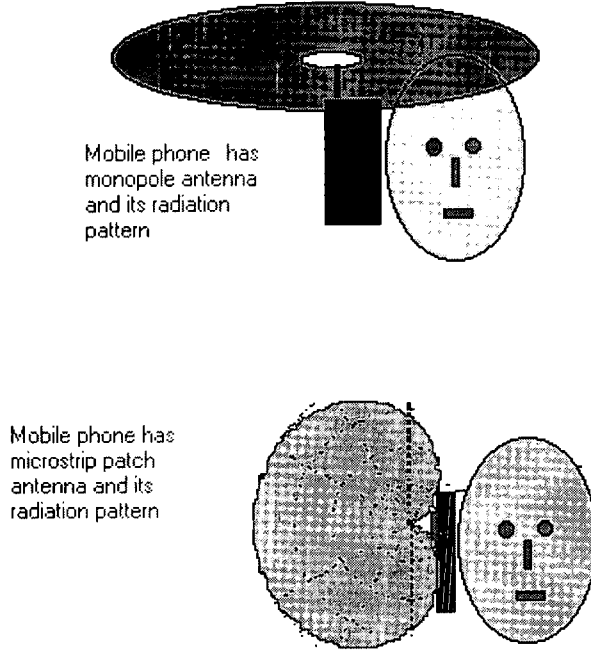


Figure 5.2: Radiation pattern that EM emitted by monopole antenna and microstrip antenna



University of Moratuwa, Sri Lanka.
Electronic Theses & Dissertations
www.lib.mrt.ac.lk

References

- [1] I. J. Dayawansa ,G.T.F..De Silva, “*Electromagnetic effects due to cellular phones*”, Paper 1999.
- [2] Prof. J. H. Moulder “*Cellular phone antennas and human health*”, Apr-2000, <http://www.mcw.edu/gcrc/cop/cell-phone-health-FAQ/toc.html>
- [3] C.C. Johnson, C.H. Durney & H.Massoudi, “*Long wave length electromagnetic power absorption in prolate spheroidal model of man & animals*”, IEEE Trans.Micro.Theo.Tech.,vol MMT-23,Sept.1975,pp. 739-747.
- [4] C. H. Durney, C.C.Johnson & H.Massoudi, , “*Long wave length analysis of plane wave irradiation of a prolate spheroidal model of man*”,IEEE Trans.Micro.Theo.Tech.,vol MMT-23, Feb.1975, pp. 246-253.
- [5] R. J. Spiegal, “*A review of numerical models for predicting the energy deposition and resultant thermal response of humans exposed to electromagnetic fields*”, IEEE Trans.Micro.Theo.Tech.,vol MMT-32, Aug.1984, pp. 730-746.
- [6] Ronald W. P. King,  www.lib.mrt.ac.lk “*Field and Currents in the Organs of the human body when Exposed to power lines and VLF Transmitters*”, IEEE Trans.Biomedical Eng.,vol 45, Apr.1998, pp. 520-530.
- [7] Dr.Henry Lai , Dr.Narendra Singh “*Neurological effects of radio frequency Electromagnetic Radiation Relating to wireless communication Technology*”, 1997, <http://www.electric-words.com/laisingh/neural1.html>
- [8] Prof. H. Chiang, “*EMF Health – effects Research*”, Nov.1999, <http://www.electric-words.com/asia/Chiang1.html>
- [9] Dr. W. R. Adey, “*Cell and Molecular Biology associated with radiation fields of Mobile telephones*”, [hppt://www.electric-words.com/adey/adeyoverview1.html](http://www.electric-words.com/adey/adeyoverview1.html)
- [10] Australian Communications Authority, “*EMR regulatory arrangements for manufacturers and importers of hand-held devices*”, May 2000, [hppt://www.sma.gov.au/standards/emrfaq%20hand-held.html](http://www.sma.gov.au/standards/emrfaq%20hand-held.html)
- [11] Mathew N. O. Sadiku , “*Numerical Techniques in Electromagnetics*”,1987
- [12] J. M. Osepchuk, “*Biological Effects of Electromagnetic Radiation*”. New York: IEEE Press,1983.

- [13] R. Jongakiem, “*Electromagnetic absorption in biological bodies*,” M.Sc. Thesis, Dept. of Electrical and Computer Engineering., Florida Atlantic Univ., Boca Raton, Aug.1988.
- [14] O. P. Gandhi, “*Electromagnetic Absorption in an inhomogeneous model of man for realistic exposure conditions*”, Bio- electromagnetics, vol.3,1982, pp . 81-90
- [15] O. P. Gandhi, et. Al., “*Part – body and multibody effects on absorption of radio – frequency electromagnetic energy by animals and by models of man*,” Radio Science, vol. 14, no. 6S, Nov.-Dec.,1979,pp15-21.
- [16] M. J. Hagmann, O.P. Gandhi, and C. H. Durney, “*Numerical calculation of electromagnetic energy deposition for a realistic model of man*,” IEEE Trans. Micro. Theo. Tech., vol. MTT-27,no. 9, Sept. 1979, pp. 804-809.
- [17] Australian Communications Authority, *EMR regulatory arrangements for manufacturers and importers of hand-held devices*, May 2000, [hppt://www.sma.gov.au/standards/emrfaq%20hand-held.html](http://www.sma.gov.au/standards/emrfaq%20hand-held.html)
- [18] D. E.Livesay & K. M.Chen, *Electromagnetic fields induced inside arbitrary shaped biological bodies*, IEEE Trans. Micro.Theo.Tech., vol. MMT-22,no.12,Dec.1974,pp.1273-1280
- [19] Yoshiaki Watanabe, Toshiyuki Tanaka, Masao Taki and So-ichi Watanabe, IEEE Trans. Micro.Theo.Tech., vol. 48, no.11, Nov. 2000, pp.2126-2132
- [20] W. G. calton and N. E. Evans, *Numerical analysis of body worn UHF antenna systems*, Electronics and Communications Engineering Journal, April 2001
- [21] Young-Min Jo, http://ee.fit.edu/electrical/asl_page/journal/report17/report17.htm
- [22] K. R. Carver and J. W. Mink, "Microstrip Antenna Technology", IEEE Trans. on Ant & Prop, vol. AP-29, No. 1, Jan. 1981
- [23] Deschamps and Y. T .Lo, D. Solomon, "Theory and Experimental on Microstrip Antennas", IEEE Trans. on Ant. & Prop. Vol. AP-27, No.2. March 1979
- [24] W. F. Richards, Y. T. Lo, "An Improved Theory for Microstrip Antennas and Applications", IEEE Trans. on Ant.& Prop. Vol. AP-29, No.1, Jan. 1981
- [25] E. H. Newman and P. Tulyathan, "Analysis of Microstrip Antennas Using Moment Methods", IEEE Trans. on Ant. & Prop. Vol. AP-29,No.1, Jan 1981

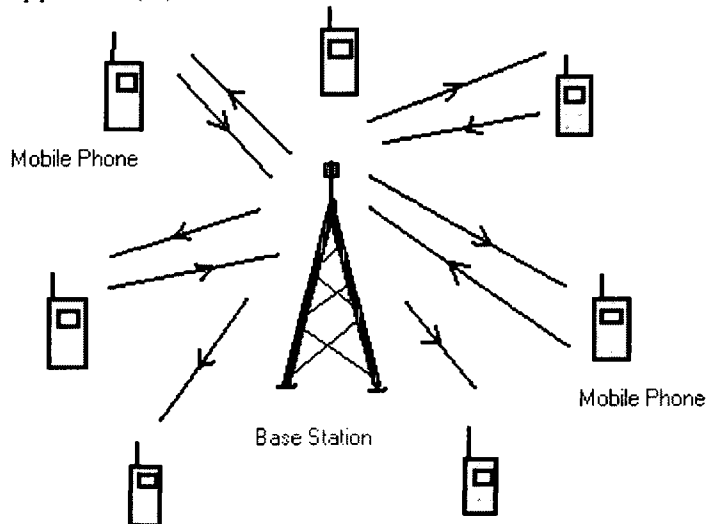
- [26] J. R. James ,"*Microstrip Antenna Theory and Design*", IEE Electromagnetic wave series , Pregrinus Ltd,1986
- [27] A. G. Derneyd, "*Linearly Polarized Microstrip Antennas*", IEEE Trans. Ant & Prop, 1976, pp846-851
- [28] R. Marg and A. F. Jacob, "*Finite ground plane effects on the radiation pattern of small microstrip arrays*", IEE Proc.-Microw. Antenna Propag. Vol. 147, No.2, April 2000
- [29] C. A. Balanis, "*Antenna Theory Analysis and design*" , John Wileys & Sons,inc,1982



University of Moratuwa, Sri Lanka.
Electronic Theses & Dissertations
www.lib.mrt.ac.lk

Appendix

Appendix (A)



Cellular Environment University of Moratuwa, Sri Lanka.
www.lib.mrt.ac.lk

Appendix (B)

BRAIN2() – calculation of EM radiation absorb by the human brain using MOM

```
function brain2(nn)
ncell=2*(nn^3);
h=.1/real(nn);
nn2=nn*2;
sig=1.29;
raw=1050.;
f=0.9e9;
w=2.*pi*f;
epso=(1.e-9)/(36.*pi);
```

```

eps=50.11*epso;
[v,x]=geometry(nn);
for n=1:ncell
    tau(n)=sig+i*w*(eps-epso);
end
[g1]=green(x,v,tau,nn);
[g2]=inv(g1);
for ics=1:6
    if ics==1
        e0=87.
    else
        e0=100.+(ics-2)*100.;
    end
    ve0(ics)=e0;
    [ei]=material(e0,nn);
    [e]=(g2)*(-ei)';
    for n=1:nn2
        sax(n)=0.;
        say(n)=0.;
        saz(n)=0.;
        htx(n)=0.;
        hty(n)=0.;
        htz(n)=0.;
    end
    n=0;
    spow=0.;
    shta=0.;
    for jj=1:nn
        for ii=1:nn2
            for kk=1:nn
                n=n+1;

                    pow=(abs(e(n)))^2+(abs(e(n+ncell)))^2+(abs(e(n+2*ncell)))^2;
                    sa=(sig/raw)*pow;
                    sar(n)=sa;
                    hta(n)=.5*sig*pow*1.e-3;

                    ssar(ii,jj,kk)=sa;
                    spow=spow+sa;
                    shta=shta+hta(n);
                    sax(ii)=sax(ii)+sa;
                    say(jj+nn)=say(jj+nn)+sa;
                    j1=nn-jj+1;
                    say(j1)=say(j1)+sa;
                    saz(kk+nn)=saz(kk+nn)+sa;
                    k1=nn-kk+1;

```



```

        saz(k1)=saz(k1)+sa;
    end
end
e0
sar;
max(sar,[],2)
mean(sar,2)
hta;
max(hta,[],2)
mean(hta,2)
sam=-.000001;
for ii=1:nn2
cd(ii)=real(ii)*h;
if sax(ii) > sam
    sam=sax(ii);
end
if say(ii) > sam
    sam=say(ii);
end
if saz(ii) > sam
    sam=saz(ii);
end
end
for ii=1:nn2
sax(ii)=sax(ii)/sam;
say(ii)=say(ii)/sam;
saz(ii)=saz(ii)/sam;
end
plot(cd,sax,cd,say,cd,saz,cd,sax,'rx',cd,say,'r+',cd,saz,'r*')
title('Relative Energy Absorbed ')
text(.025,.95,'Frequency 900 Mhz.')
text(.025,.90,'No. cells 1000 ')
text(.025,.85,'Fld. Int. V/m')
xlabel('x- X axis, + Y - axis, * Z - axis (m.)')
ylabel('Relative Energy Absorbed')
input z
power(ics)=spow/nccell;
tht(ics)=shta;
r(ics)=power(ics)/tht(ics);
end
ve0
power
tht
r
input zz;

```



```

plot(ve0,power,'r-',ve0,power,'r+')
title('Graph of Energy Absorbed vs. Field Intensity')
text(55.,19.,'Frequency 900 Mhz.')
text(55.,17.,'No cells 1000')
xlabel('Field Intensity (V/m)')
ylabel('Energy Absorbed (W/kg.)')

```

Appendix (C)

SKTIS() –calculation of EM radiation absorb by the human brain and Skull using MOM

```

function sktis(nn)
ncell=2*(nn^3);
h=.1/real(nn);
nn2=nn*2;
sig=1.29;
sig1=0.45;
raw=1050.;
raw1=1000;
f=0.9e9;
w=2.*pi*f;
eps0=(1.e-9)/(36.*pi);
eps=50.11*eps0;
[v,x]=geometry(nn);
n=0;
for ii=1:nn2
    for jj=1:nn
        for kk=1:nn
            n=n+1;
            if (ii>1 | ii<nn2) & (jj<nn) & (kk<nn)
                tau(n)=sig+i*w*(eps-eps0);
            else
                tau(n)=sig1*i*w*(eps-eps0);
            end
        end
    end
end

```



```

[g1]=green(x,v,tau,nn);
[g2]=inv(g1);
for ics=1:6
    if ics==1
        e0=87.
    else
        e0=100.+(ics-2)*100.;
    end
    ve0(ics)=e0;
    [ei]=material(e0,nn);
    [e]=(g2)*(-ei)';
    ei
    for n=1:nn2
        sax(n)=0. ;
        say(n)=0. ;
        saz(n)=0. ;
        htx(n)=0. ;
        hty(n)=0. ;
        htz(n)=0. ;
    end
    n=0;
    spow=0. ;
    shta=0. ;
    for jj=1:nn
        for ii=1:nn2
            for kk=1:nn
                n=n+1;

                pow=(abs(e(n)))^2+(abs(e(n+ncell)))^2+(abs(e(n+2*ncell)))^2;
                if (ii>1 | ii<nn2) & (jj<nn) & (kk<nn)
                    sa=(sig/raw)*pow;
                    sar(n)=sa;
                    hta(n)=.5*sig*pow*1.e-3;

                else
                    sa=(sig1/raw1)*pow;
                    sar(n)=sa;
                    hta(n)=.5*sig1*pow*1.e-3;
                end
                ssar(ii,jj,kk)=sa;
                spow=spow+sa;
                shta=shta+hta(n);
                sax(ii)=sax(ii)+sa;
                say(jj+nn)=say(jj+nn)+sa;
                j1=nn-jj+1;

```



```

say(j1)=say(j1)+sa;
saz(kk+nn)=saz(kk+nn)+sa;
k1=nn-kk+1;
saz(k1)=saz(k1)+sa;
end
end
e0
ei
sar;
max(sar,[],2)
mean(sar,2)
hta
max(hta,[],2)
mean(hta,2)
sam=-.000001;
for ii=1:nn2
cd(ii)=real(ii)*h;
if sax(ii) > sam
    sam=sax(ii);
end
if say(ii) > sam
    sam=say(ii);
end
if saz(ii) > sam
    sam=saz(ii);
end
end
for ii=1:nn2
    sax(ii)=sax(ii)/sam;
    say(ii)=say(ii)/sam;
    saz(ii)=saz(ii)/sam;
end
plot(cd,sax,cd,say,cd,saz,cd,sax,'rx',cd,say,'r+',cd,saz,'r*')
title('Relative Energy Absorbed ')
text(.025,.95,'Frequency 900 Mhz.')
text(.025,.90,'No. cells 1000 ')
text(.025,.85,'Field. Int. V/m')
xlabel('x- X axis, + Y - axis, * Z - axis (m.)')
ylabel('Relative Energy Absorbed')
input z
power(ics)=spow/nccell;
tht(ics)=sht;
r(ics)=power(ics)/tht(ics);
end
ve0

```



```

power
tht
r
input zz;
plot(ve0,power,'r-',ve0,power,'r+')
title('Graph of Energy Absorbed vs. Field Intensity')
text(55.,19.,'Frequency 900MHz.')
text(55.,17.,'No cells 1000')
xlabel('Field Intensity (V/m)')
ylabel('Energy Absorbed (W/kg.)')

```

Appendix (D)

SKTIS1() – calculation of EM radiation absorb by the human Brain, Skull and ear using MOM

```

function sktis1(nn)
ncell=2*(nn^3);
h=.05/real(nn);
nn2=nn*2;
sig=1.29;
sig1=0.45;
raw=1050.;
raw1=1000;
f=0.9e9;
w=2.*pi*f;
eps0=(1.e-9)/(36.*pi);
eps=50.11*eps0;
[v,x]=geometry(nn);
n=0;
for ii=1:nn2
    for jj=1:nn
        for kk=1:nn
            n=n+1;
            if (ii>1 | ii<nn2) & (jj<nn) & (kk<nn)
                tau(n)=sig+i*w*(eps-eps0);
            elseif (ii==1 & ii==nn*2) & (jj==nn) & (kk==nn)
                tau(n)=sig1+i*w*(eps-eps0);
            else
                tau(n)=sig1*i*w*(eps-eps0);
            end;

```



```

    end
end
end
[g1]=green(x,v,tau,nn);
[g2]=inv(g1);
for ics=1:6
if ics==1
    e0=87.
else
    e0=100.+(ics-2)*100.;
end
ve0(ics)=e0;
[ei]=material(e0,nn);
[e]=(g2)*(-ei)';
ei
for n=1:nn2
    sax(n)=0.;
    say(n)=0.;
    saz(n)=0.;
    htx(n)=0.;
    hty(n)=0.;
    htz(n)=0.;
end
n=0;
spow=0.;
shta=0.;
for jj=1:nn
    for ii=1:nn2
        for kk=1:nn
            n=n+1;
            pow=(abs(e(n)))^2+(abs(e(n+ncell)))^2+(abs(e(n+2*ncell)))^2;
            if (ii>1 | ii<nn2) & (jj<nn) & (kk<nn)
                sa=(sig/raw)*pow;
                sar(n)=sa;
                hta(n)=.5*sig*pow*1.e-3;
                elseif (ii==1 & ii==nn*2) & (jj==nn) & (kk==nn)
                    sa=(sig/raw)*pow;
                    sar(n)=sa;
                    hta(n)=.5*sig*pow*1.e-3;
                else
                    sa=(sig1/raw1)*pow;
                    sar(n)=sa;
                    hta(n)=.5*sig1*pow*1.e-3;
                end;
            ssar(ii,jj,kk)=sa;

```



```

spow=spow+sa;
shta=shta+hta(n);
sax(ii)=sax(ii)+sa;
say(jj+nn)=say(jj+nn)+sa;
j1=nn-jj+1;
say(j1)=say(j1)+sa;
saz(kk+nn)=saz(kk+nn)+sa;
k1=nn-kk+1;
saz(k1)=saz(k1)+sa;

end
end
end
e0
ei
sar
hta
sam=-.000001;
for ii=1:nn2
cd(ii)=real(ii)*h;
if sax(ii) > sam
    sam=sax(ii);
end
if say(ii) > sam
    sam=say(ii);
end
if saz(ii) > sam
    sam=saz(ii);
end
end
for ii=1:nn2
    sax(ii)=sax(ii)/sam;
    say(ii)=say(ii)/sam;
    saz(ii)=saz(ii)/sam;

end
plot(cd,sax,cd,say,cd,saz,cd,sax,'rx',cd,say,'r+',cd,saz,'r*')
title('Relative Energy Absorbed ')
text(.025,.95,'Frequency 900 Mhz.')
text(.025,.90,'No. cells 1000 ')
text(.025,.85,'Field. Int. V/m')
xlabel('x- X axis, + Y - axis, * Z - axis (m.)')
ylabel('Relative Energy Absorbed')
input z
power(ics)=spow/nCELL;
tht(ics)=shta;

```



```

r(ics)=power(ics)/tht(ics);
end
ve0
power
tht
r
input zz;
plot(ve0,power,'r-',ve0,power,'r+')
title('Graph of Energy Absorbed vs. Field Intensity')
text(55.,19.,'Frequency 900MHz.')
text(55.,17.,'No cells 1000')
xlabel('Field Intensity (V/m)')
ylabel('Energy Absorbed (W/kg.)')

```

Appendix (E)

GREEN()



University of Moratuwa, Sri Lanka.
Electronic Theses & Dissertations
www.lib.mrt.ac.lk

```

function [g1]=green(x,v,tau,nn)
f=0.9e9;
eps0=(1.e-9)/(36*pi);
u0=(4.e-7)*pi;
w=2*pi*f;
k0=w*((u0*eps0)^(.5));
c=-j*w*u0*k0;
c1=-2*j*w*u0/(3*(k0^2));
c2=3*j*w*eps0;
ncell=2*(nn^3);
for p=1:3
    for q=1:3
        x1=(p-1)*ncell;
        for m=1:ncell
            x1=x1+1;
            x2=(q-1)*ncell;
            for n1=1:ncell
                x2=x2+1;
                if m==n1
                    an=(3*v(n1))/(4*pi)^(1/3);
                    c3=j*k0*an;
                    c4=tau(n1)/c2;
                    gg=c1*tau(n1)*((1+c3)*exp(-c3)-1)-(1+c4);

```

```

if p==q
    del=1;
    g1(x1,x2)=del*gg;
else
    del=0;
    g1(x1,x2)=del*gg;
end
else
    d=(x(1,n1)-x(1,m))^2+(x(2,n1)-(x(2,m))^2+(x(3,n1)-x(3,m))^2;
    d=d^(.5);
    if d==0
        s='distance same'
    end
    amn=k0*d;
    if p==q
        del=1;
    else
        del=0;
    end
    c3=(c*tau(n1)*v(n1)*exp(-l*amn))/(4*pi*amn^3);
    cs=(x(p,m)-x(p,n1))*(x(q,m)-x(q,n1))/(d^2);
    g1(x1,x2)=c3*((amn-l*i*amn)*del)+cs*(3*amn^2+3*i*amn);
    end
end
end
end

```



Appendix (F)

GEOMETRY()

```
function [v,x]=geometry(nn)
h=.1/nn;
vv=h^3;
n2=2*nn;
n=0;
for jj=1:nn
    for ii=1:n2
        for kk=1:nn
            n=n+1;
            v(n)=vv;
            x(1,n)=(ii-1)*h+h/2;
            x(2,n)=(jj-1)*h+h/2;
            x(3,n)=(nn-(kk-1))*h-h/2;
        end
    end
end
```



University of Moratuwa, Sri Lanka.
Electronic Theses & Dissertations
www.lib.mrt.ac.lk

Appendix (G)

MATERIAL()

```
function [ei]=material(e0,nn)
ncell=2*(nn^3);
n2=nn*2;
h=.1/nn;
ncell3=ncell*3;
for ii=1:ncell3
    ei(ii)=0;
end
n=0;
for jj=1:nn
    for ii=1:n2
        for kk=1:nn
            n=n+1;
            ei(n)=0;
            if ii==1
                ei(n)=e0*.03/((.03^2+(jj*h)^2)^.5);
            end
            ei(n+ncell)=0;
            ei(n+2*ncell)=0;
        end
    end
end
```

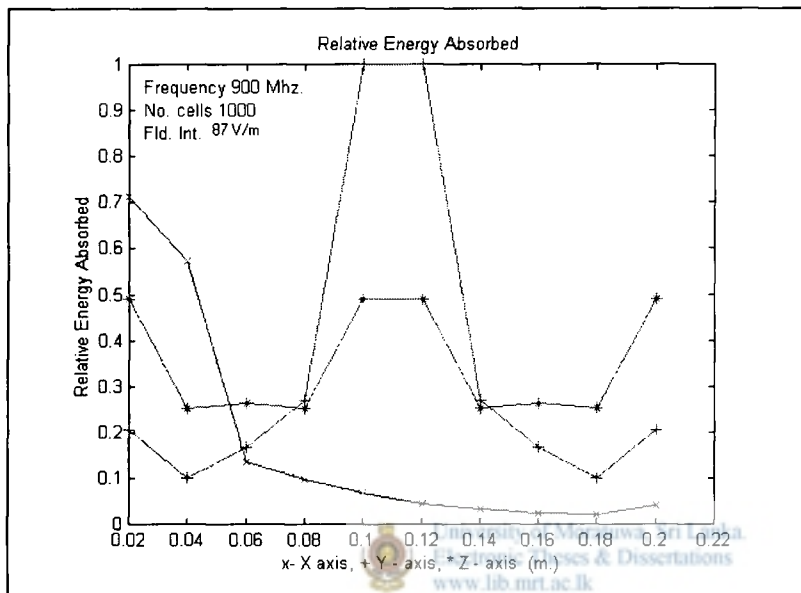


Appendix (H)

Using brain2.m Matlab program the graphical outputs

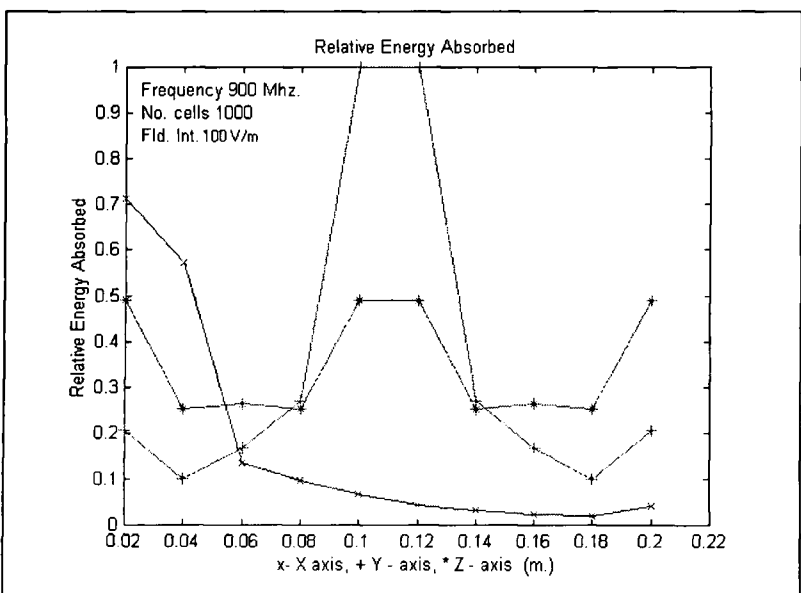
When $E_0=87 \text{ V/m}$

The energy absorption (considering brain tissues only) along X, Y, Z-axis due to entering EM radiations



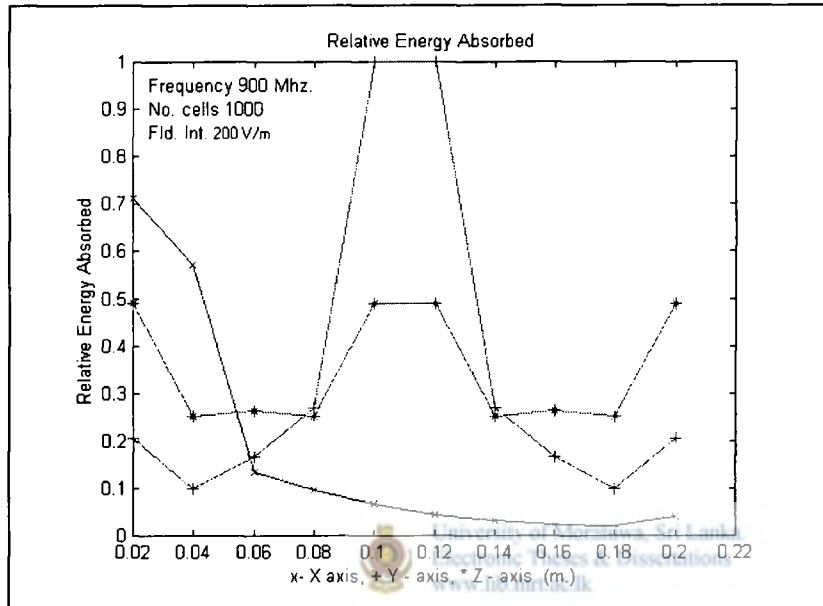
When $E_0=100 \text{ V/m}$

The energy absorption (considering brain tissues only) along X, Y, Z-axis due to entering EM radiations

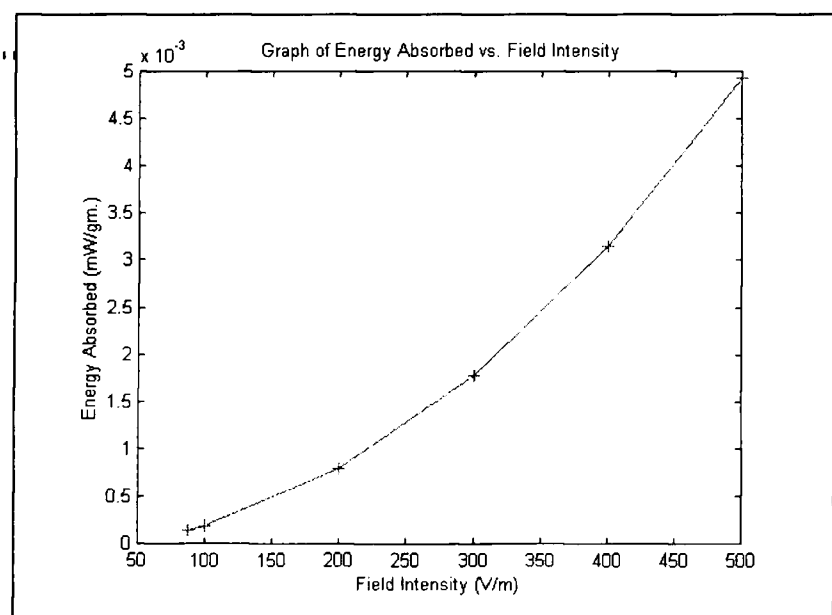


When $E_0=200$ V/m

The energy absorption (considering brain tissues only) along X, Y, Z-axis due to entering EM radiations



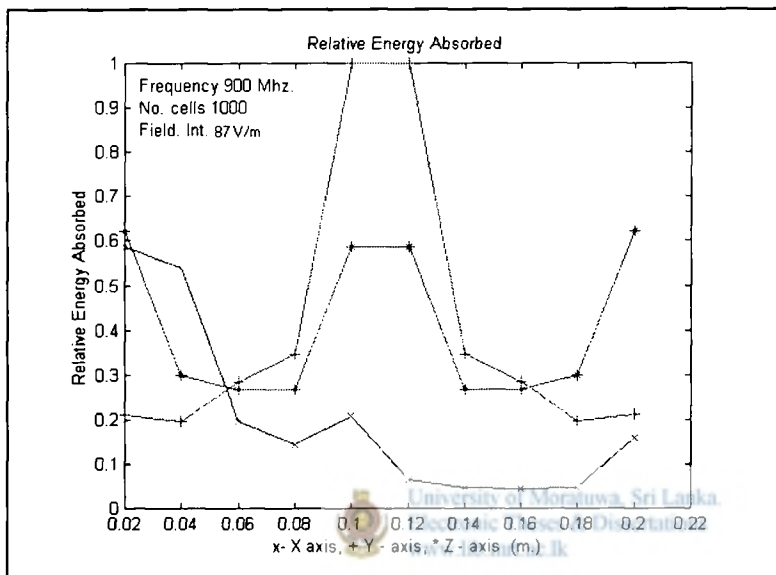
SAR variation due to entering EM radiations



Using sktis.m matlab program the graphical outputs

When $E_0=87 \text{ V/m}$

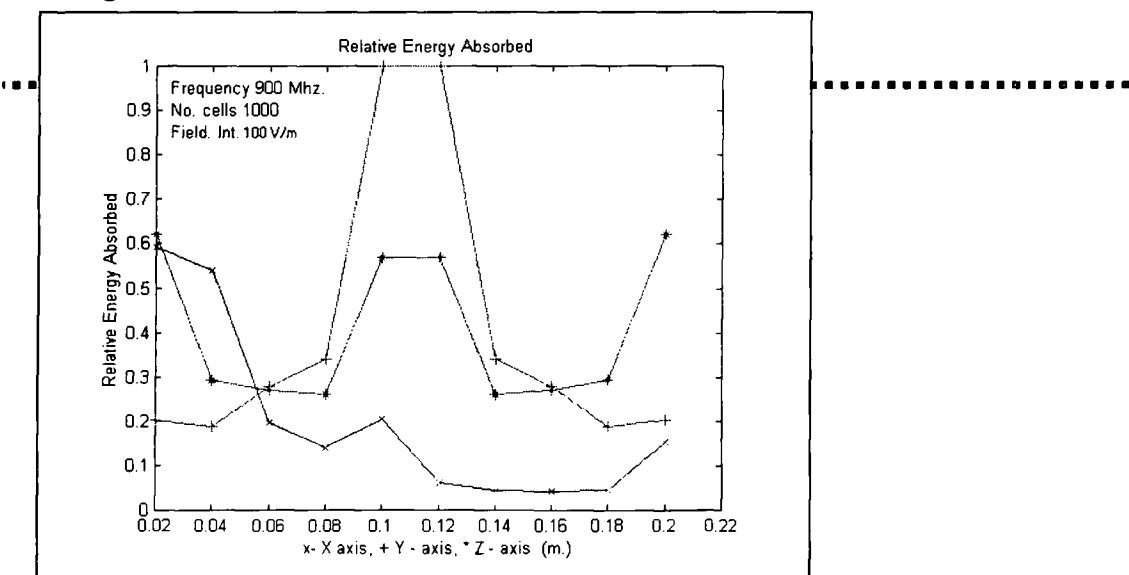
The energy absorption (considering brain tissues, skull) along X, Y, Z-axis due to



entering EM radiations

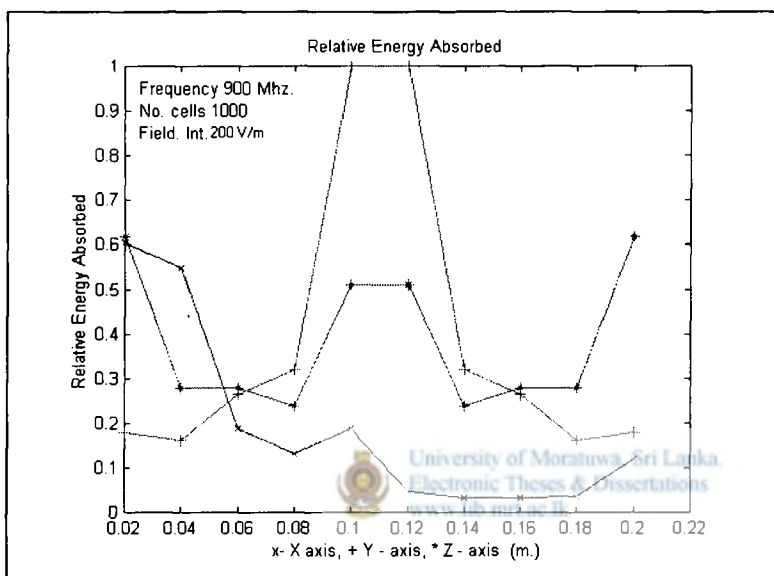
When $E_0=100 \text{ V/m}$

**The energy absorption (considering brain tissues, skull) along X, Y, Z-axis due to
entering EM radiations**



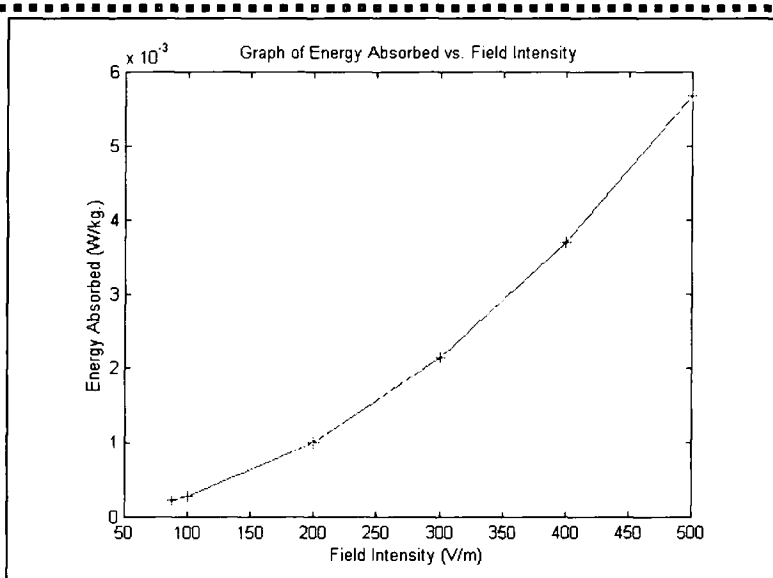
When $E_0=200$ V/m

The energy absorption (considering brain tissues, skull) along X, Y, Z-axis due to entering EM radiations



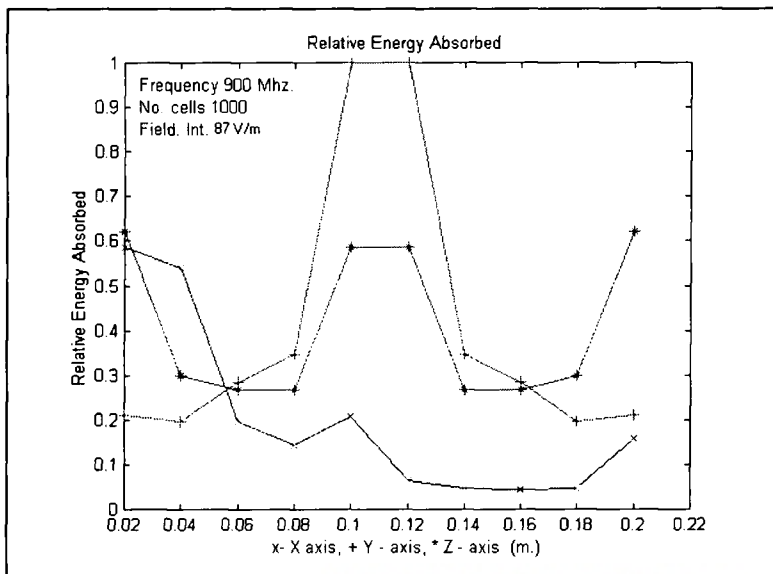
SAR variation due to entering EM radiations

Using sktis1.m Matlab program the graphical outputs



When $E_0=87 \text{ V/m}$

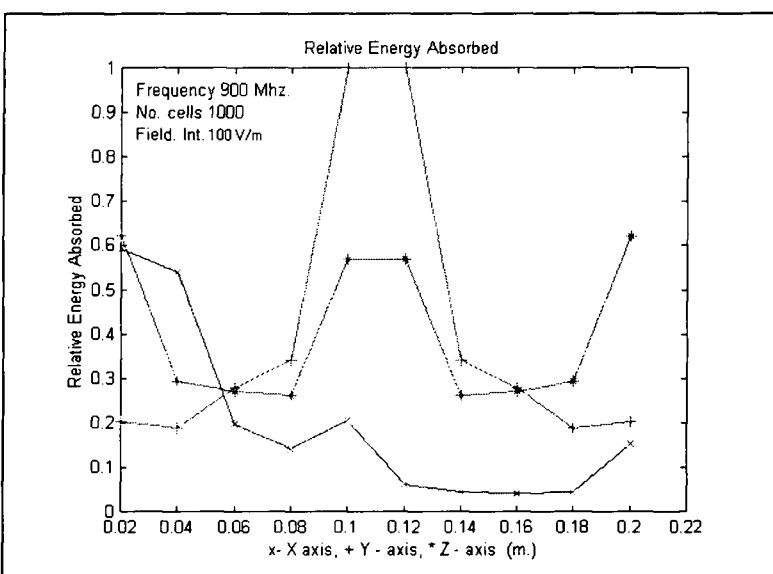
The energy absorption (considering brain tissues, skull and ear as a tissue) along X, Y, Z-axis due to entering EM radiations



University of Moratuwa, Sri Lanka.
Electronic Theses & Dissertations
www.lib.mrt.ac.lk

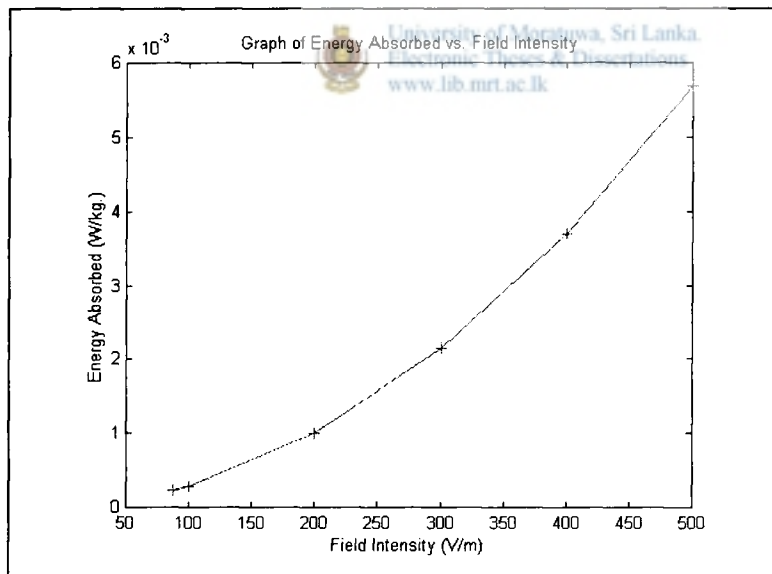
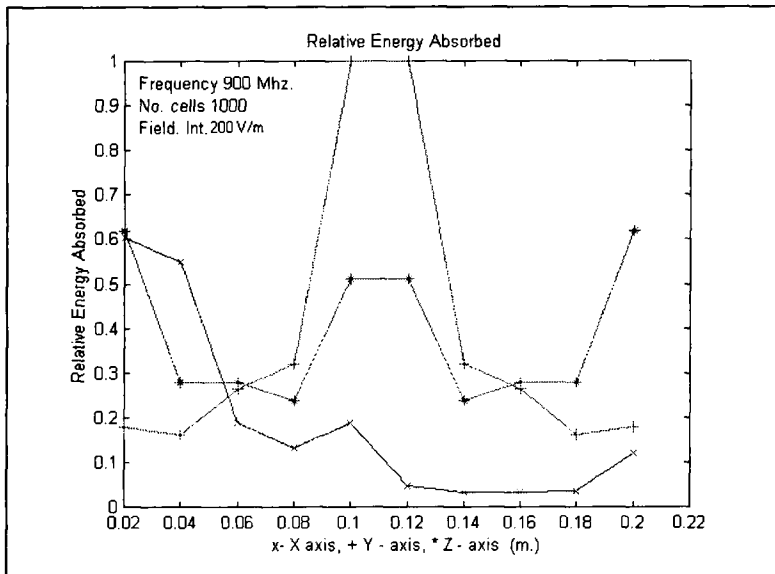
When $E_0=100 \text{ V/m}$

The energy absorption (considering brain tissues, skull and ear as a tissue) along X, Y, Z-axis due to entering EM radiations



When $E_0=200 \text{ V/m}$

The energy absorption (considering brain tissues, skull and ear as a tissue) along X, Y, Z-axis due to entering EM radiations



SAR variation due to entering EM radiations

Appendix (I) –Method of Moment

$$\nabla \times E^S = -J_{eq} - j\omega H^S \quad \dots \dots \dots \quad (4a)$$

where E_s , H_s and J_{eq} are all in phasor (complex) form. Elimination of E_s or H_s in equation (4) leads to

$$\nabla \times \nabla \times E^S - k_0^2 E^S = -j\omega\mu_0 J_{eq} \quad \dots \dots \dots \quad (5a)$$

where $k_0^2 = \omega^2 \mu_0 \epsilon_0$. The solutions to equation (5) are

and hence from 4(b)

where

and the free space Green's function,



University of Moratuwa, Sri Lanka.
Electronic Theses & Dissertations
www.lib.mrt.ac.lk

is the free-space scalar Green's function. By the operator $\nabla\nabla_{\perp}$, we mean that $\nabla\nabla_{\perp}A = \nabla(\nabla_{\perp}A)$. It is evident from eq.(6) that E_s and H_s depend on J_{eq} is an infinitesimal, elementary source at r' pointed in the x direction so that

the corresponding vector potential is obtained from eq. (7) as

$$A = \mu_0 G_0 (r, r') a_x \dots \quad (10)$$

If $G_{0x}(r, r')$ is the electric field produced by the elementary source, then $G_{0x}(r, r')$ must satisfy

and has the solution

$G_{0x}(r,r')$ is referred to as a free-space vector Green function with a source pointed in the x direction. We could also have $G_{0y}(r,r')$ and $G_{0z}(r,r')$ corresponding to infinitesimal, elementary sources pointed in the y and z direction, respectively. We now introduce a dyadic function which can store the three vector Green functions $G_{0x}(r,r')$, $G_{0y}(r,r')$ and $G_{0z}(r,r')$, i.e.

$G_0(r, r')$ is a solution to the dyadic differential equation,

This is called free-space dyadic Green's function. It is a solution to the dyadic differential equation

Where \bar{I} denotes the unit dyad (or idem factor).

The physical meaning of $G_0(r,r')$ is rather obvious. $G_0(r,r')$ is the electric field at a field point r due to an infinitesimal source at r' .

From equations (5a) and (13), the solution of E is evidently,

$$E^s(r) = -j\omega\mu_0 \int G_0(r, r') J_{eq}(r') dv' lib.mrt.ac.jp(15)$$

$G_0(r, r')$ has a singularity of the order $|r - r'|^3$, the integral in eq. (14) diverges if the field points r is inside the volume V of the body (or source region). This difficulty is overcome with by excluding a small volume approach zero. The process entails defining the principal value (P V) and adding a correction term needed to yield the correct solution.

$$E^s(r) = PV \int J_{eq}(r) G_0(r, r') . dv' + [E^s(r)] \quad \dots \dots \dots (16)$$

The correction term has been evaluated to be $-J_{eq} / j_3 \omega \epsilon_0$ so that

$$E^s(r) = PV \int J_{eq}(r) G_0(r, r') . dv' + J_{eq}(r) / (3j\omega\varepsilon_0) \quad \dots \dots \dots (17)$$

The total electric field inside the body is the sum of the incident field E^i and scattered field E^s ,

Combining eqs. (2), (16) and (17) gives the desired tensor integral equation for $E(r)$:

$$\left(1 + \frac{\tau}{3\gamma_{\alpha\epsilon_0}}\right) E(r) - PV \int \tau_e E(r') G_0(r, r') dv' = E^i(r) \dots \dots \dots (19)$$

Appendix (J) _FDTD Method

First is the Hooke's law with the thermal stress term,

$$\frac{\partial \sigma_{xx}}{\partial t} = (\lambda + 2\mu) \frac{\partial v_x}{\partial x} + \lambda \frac{\partial v_y}{\partial y} + \lambda \frac{\partial v_z}{\partial z} - \alpha(3\lambda + 2\mu) \frac{\partial T}{\partial t} \quad \quad \quad \quad (ii)$$

$$\frac{\partial \sigma_{yy}}{\partial t} = (\lambda) \frac{\partial v_x}{\partial x} + (\lambda + 2\mu) \frac{\partial v_y}{\partial y} + \lambda \frac{\partial v_z}{\partial z} - \alpha(3\lambda + 2\mu) \frac{\partial T}{\partial t} \quad(iii)$$

$$\frac{\partial \sigma_{zz}}{\partial t} = (\lambda) \frac{\partial v_x}{\partial x} + (\lambda) \frac{\partial v_y}{\partial y} + (\lambda + 2\mu) \frac{\partial v_z}{\partial z} - \alpha(3\lambda + 2\mu) \frac{\partial T}{\partial t} \quad(iv)$$

And the second is the equations of the motion

$\frac{\partial \sigma_{yz}}{\partial t} = \mu \left(\frac{\partial v_y}{\partial z} + \frac{\partial v_z}{\partial y} \right) \dots$ University of Moratuwa, Sri Lanka.
 Electronic Theses & Dissertations
www.lib.mrt.ac.lk (vi)

$$\rho \frac{\partial v_y}{\partial t} = \left(\frac{\partial \sigma_{xy}}{\partial x} + \frac{\partial \sigma_{yy}}{\partial y} + \frac{\partial \sigma_{yz}}{\partial z} \right) \quad \dots \dots \dots \quad (ix)$$

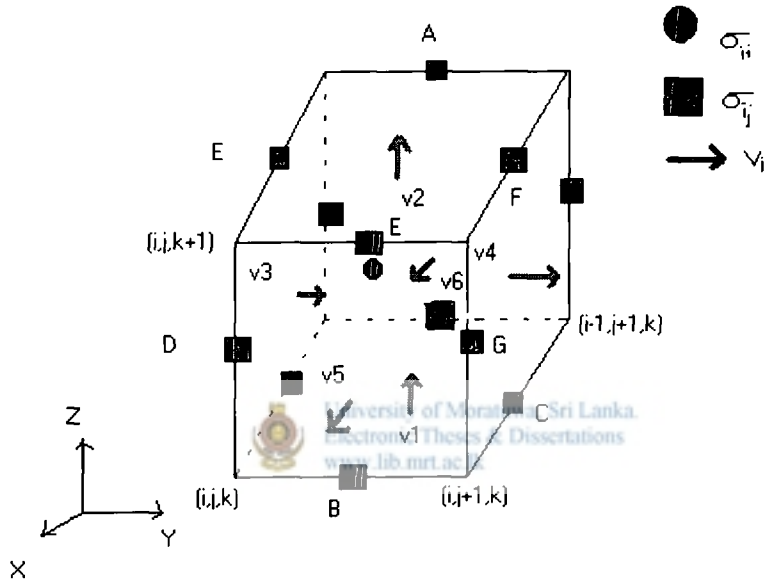
$$\rho \frac{\partial v_x}{\partial t} = \left(\frac{\partial \sigma_{zx}}{\partial x} + \frac{\partial \sigma_{yz}}{\partial y} + \frac{\partial \sigma_{zz}}{\partial z} \right) \quad \dots \dots \dots \quad (x)$$

Where (σ_{ij}) is the stress tensor, v_i is the particle velocity, λ and μ are the Lame's constants, α is the coefficient of linear thermal expansion, and ρ is the mass density of the tissue.

We assume that the temperature rise T is given by

Where $C_h(x,y,z)$ is the specific heat of the tissue at the point (x,y,z) and t_0 is the pulse duration. These two sets of governing equations are discretized to the FDTD form.

Following Yee's notation [20], a point in a cartesian grid is expressed as



Staggered cell geometry for elastic-wave computation

and any field value F of discrete space and time is expressed as

Where $A = \sigma_{zx}(i-1, j+1/2, k+1)$ and $v2 = v_z(i-1/2, j+1/2, k+1)$

$$B = \sigma_{zx}(i, j+1/2, k) \quad v4 = v_y(i-1/2, j+1, k+1/2)$$

$$C = \sigma_{zy}(i-1/2, j+1, k) \quad v5 = v_x(i, j+1/2, k+1/2)$$

$$D = \sigma_{xy}(i, j, k+1/2)$$

$$E = \sigma_{zx}(i, j+1/2, k+$$

$$F = \sigma_{yz}(i-1/2, j+1, k+$$

$$G = \sigma_{xy}(i, j+1, k+1/2)$$

Where Δt is time increment, and i, j, k, n are integers. The staggered cell for the FDTD method for elastic waves is shown in above figure.

The field equations are discretized using Yee's leapfrog scheme with centered finite difference, and then the update equations are obtained. From equation ii,v,viii we have

$$\begin{aligned} \sigma_{xx}^{n+1}(i+\frac{1}{2}, j+\frac{1}{2}, k+\frac{1}{2}) &= \sigma_{xx}^{n-1}(i+\frac{1}{2}, j+\frac{1}{2}, k+\frac{1}{2}) + \frac{(\lambda+2\mu)\Delta t}{\Delta x} [v_x^{n-(1/2)}(i+1, j+\frac{1}{2}, k+\frac{1}{2}) \\ &\quad - v_x^{n-(1/2)}(i, j+\frac{1}{2}, k+\frac{1}{2})] + \frac{\lambda\Delta t}{\Delta y} [v_y^{n-(1/2)}(i+1, j+1, k+\frac{1}{2}) - v_y^{n-(1/2)}(i+\frac{1}{2}, j, k+\frac{1}{2}) \\ &\quad + \frac{\lambda\Delta t}{\Delta z} [v_z^{n-(1/2)}(i+\frac{1}{2}, j+\frac{1}{2}, k+1) - v_z^{n-(1/2)}(i+\frac{1}{2}, j+\frac{1}{2}, k+\frac{1}{2})] \\ &\quad - \alpha(3\lambda+2\mu)\Delta t \frac{\partial T(i+\frac{1}{2}, j+\frac{1}{2}, k+\frac{1}{2})}{\partial t}] \end{aligned} \quad ..(xiv)$$

$$\begin{aligned} \sigma_{xy}^n(i, j, k+\frac{1}{2}) &= \sigma_{xy}^{n-1}(i, j, k+\frac{1}{2}) + \frac{\mu\Delta t}{\Delta x} [v_y^{n+(1/2)}(i+\frac{1}{2}, j, k+\frac{1}{2}) - v_y^{n-(1/2)}(i-\frac{1}{2}, j, k+\frac{1}{2})] + \\ &\quad \frac{\mu\Delta t}{\Delta y} [v_x^{n-(1/2)}(i, j+\frac{1}{2}, k+\frac{1}{2}) - v_x^{n-(1/2)}(i, j-\frac{1}{2}, k+\frac{1}{2})] \end{aligned} \quad ..(xv)$$

$$\begin{aligned} v_x^{n+(1/2)}(i, j+\frac{1}{2}, k+\frac{1}{2}) &= v_x^{n-(1/2)}(i, j+\frac{1}{2}, k+\frac{1}{2}) + \frac{\Delta t}{\rho\Delta x} [\sigma_{yy}^n(i+\frac{1}{2}, j+\frac{1}{2}, k+\frac{1}{2}) - \sigma_{xx}^n(i-\frac{1}{2}, j+\frac{1}{2}, k+\frac{1}{2})] \\ &\quad + \frac{\Delta t}{\rho\Delta y} [\sigma_{xy}^n(i, j+1, k+\frac{1}{2}) - \sigma_{xy}^n(i, j, k+\frac{1}{2})] + \frac{\Delta t}{\rho\Delta z} [\sigma_{xz}^n(i, j+\frac{1}{2}, k+1) - \sigma_{xz}^n(i, j+\frac{1}{2}, k)] \end{aligned} \quad ..(xvi)$$

The source term $\partial T / \partial t$ should be derived from (xi). Instead of simply taking a time derive of (xi), we used the following functional form for this term in order to reduce higher frequency components that cannot be efficiently computed by the finite difference method:

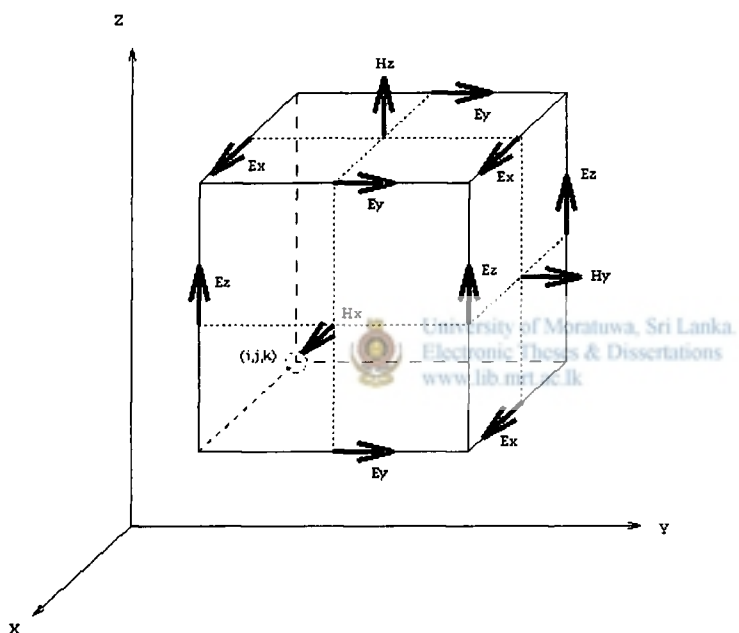
$$\frac{\partial T(x, y, z, t)}{\partial t} = \frac{SAR(x, y, z)}{2C_h(x, y, z)} \{erf(at) - erf(a(t-t_0))\} \quad ..(xvii)$$

The parameter a in (xvii) represents the steepness of the microwave pulse. We assumed $a=0.4 \times 10^6$ in the following analysis.

Elastic properties of the tissues

	Tissues	Skull
Density(ρ)[kg/m ³]	1050	1000
Specific heat(C_h)[J/kg°C]	3860	1600
Lame's constant(λ)[Gpa]	2.240	6.923
Lame's constant(μ)[Gpa]	1.052×10^{-6}	4.615
Coefficient of thermal expansion (α)[1/°C]	4.1×10^{-5}	1.06×10^{-5}

Appendix K



FDTD cell geometry with interleaved electric (E fields on edges) and magnetic (H fields on faces) fields. Note that four magnetic field vectors circulate around each electric field vector and vice versa.

Considering first a region of space without electric or magnetic current sources, the curl equations are:

and

Here E is the electric field vector (Vm^{-1}), D is electric flux density vector (Cm^{-2}), H is the magnetic field vector (Am^{-1}), B is the magnetic flux density (Wm^{-2}), J_e is the electric conduction current density (Vm^{-2}) and J_m is the equivalent magnetic conduction current density (Vm^{-2}). To account for losses due to the dissipation of fields in materials we can introduce an electric conductivity σ (Sm^{-1}) and an equivalent magnetic resistivity ρ' (Ωm^{-1}) and equate them to the field vectors above using:

and

For linear, isotropic and non-dispersive materials, there are simple relations between flux density and fields. Defining μ as magnetic permeability (Hm^{-1}) and ϵ as electric permittivity (Fm^{-1}), we can write



University of Moratuwa, Sri Lanka.
Electronic Theses & Dissertations
www.lib.mrt.ac.lk

and

Substituting equations 3-6 in equations 1 and 2, we obtain:

and

Using the explicit expression for the curl operator and setting the magnetic loss ρ' to zero, we can derive a system of scalar equations for a rectangular co-ordinate system (x,y,z) applicable to non-magnetic materials:

$$\frac{\partial H_x}{\partial t} = \frac{1}{\mu} \left(\frac{\partial E_y}{\partial z} - \frac{\partial E_z}{\partial y} \right) \quad \dots \quad (9a)$$

$$\frac{\partial H_y}{\partial t} = \frac{1}{\mu} \left(\frac{\partial E_z}{\partial x} - \frac{\partial E_x}{\partial z} \right) \quad \dots \quad (9b)$$

$$\frac{\partial H_x}{\partial t} = \frac{1}{\mu} \left(\frac{\partial E_x}{\partial y} - \frac{\partial E_y}{\partial x} \right) \quad \dots \quad (9c)$$

$$\frac{\partial E_x}{\partial t} = \frac{1}{\varepsilon} \left(\frac{\partial H_z}{\partial y} - \frac{\partial H_y}{\partial z} - \sigma E_x \right) \quad \dots \dots \dots \quad (10a)$$

$$\frac{\partial E_y}{\partial t} = \frac{1}{\varepsilon} \left(\frac{\partial H_x}{\partial z} - \frac{\partial H_z}{\partial x} - \sigma E_y \right) \quad \dots \dots \dots \quad (10b)$$

$$\frac{\partial E_z}{\partial t} = \frac{1}{\epsilon} \left(\frac{\partial H_y}{\partial x} - \frac{\partial H_x}{\partial y} - \sigma E_z \right) \quad \dots \quad (10c)$$

In the FDTD method, the time and space derivatives in equations 9 and 10 are replaced with central differences, requiring space and time interleaving of E and H. The general central difference approximations of time and space derivatives are:

Magnetic field equations

Applying equations 11 and 12 to equation 9, we can derive a set of finite difference equations for updating the magnetic field vectors. Considering equation 9a for a location (i,j,k) we can write:

$$\frac{H_x|_{i,j,k}^{n+1/2} - H_x|_{i,j,k}^{n-1/2}}{\Delta t} = \frac{1}{\mu_{i,j,k}} \left(\frac{E_y|_{i,j,k+1/2}^n - E_y|_{i,j,k-1/2}^n}{\Delta z} \right) - \left(\frac{E_z|_{i,j+1/2,k}^n - E_z|_{i,j-1/2,k}^n}{\Delta y} \right) \quad ... (13)$$

Note that at time step $n+1/2$, the new value of H_x can be directly calculated from the values of E_y and E_z at time step n and the last value of H_x (time step $n-1/2$). Rearranging equation 13 gives the explicit update equation for H_x :

$$H_x|_{i,j,k}^{n+1/2} = H_x|_{i,j,k}^{n-1/2} - \frac{\Delta t}{\Delta y, \mu_{i,j,k}} (E_y|_{i,j+1/2,k}^n - E_y|_{i,j-1/2,k}^n) + \frac{\Delta t}{\Delta z, \mu_{i,j,k}} (E_y|_{i,j,k+1/2}^n - E_y|_{i,j,k-1/2}^n) \dots (14)$$

Likewise, FDTD update equations may be derived for H_y and H_z

Electric field equations

Similarly, we can apply finite differences to equation 10, considering E_x (equation 10a) we can write:

$$\frac{E_x|_{i,j,k}^{n+1} - E_x|_{i,j,k}^n}{\Delta t} = \frac{1}{\epsilon_{i,j,k}} \left(\frac{H_z|_{i,j+1/2,k}^{n+1/2} - H_z|_{i,j-1/2,k}^{n+1/2}}{\Delta y} - \frac{H_y|_{i,j,k+1/2}^{n+1/2} - H_y|_{i,j,k-1/2}^{n+1/2}}{\Delta z} - \sigma E_x|_{i,j,k}^{n+1/2} \right). \dots (15)$$

In this case rewriting for an updated E_x at time step $n+1$ is not straightforward due to the presence of E_x at time step $n+1/2$ (rather than n or $n+1$) on the right hand side. The solution is to employ a semi implicit approximation for E_x (at $n+1/2$) by averaging of the values of E_x at n and $n+1$ and rewriting as:

$$E_x|_{i,j,k}^{n+1} = \left(\frac{1 - \frac{\sigma \Delta t}{2\epsilon}}{1 + \frac{\sigma \Delta t}{2\epsilon}} \right) E_x|_{i,j,k}^n + \left(\frac{\frac{\Delta t}{\epsilon}}{\left(1 + \frac{\sigma \Delta t}{2\epsilon} \right) \Delta y} \right) (H_z|_{i,j+1/2,k}^{n+1/2} - H_z|_{i,j-1/2,k}^{n+1/2}) - \left(\frac{\frac{\Delta t}{\epsilon}}{\left(1 + \frac{\sigma \Delta t}{2\epsilon} \right) \Delta z} \right) (H_y|_{i,j,k+1/2}^{n+1/2} - H_y|_{i,j,k-1/2}^{n+1/2}) \dots \dots (16)$$

Where ϵ and σ are specific at the cell location (i,j,k) . In practice, the multipliers on the right-hand side of equation 16 are calculating for each material type and stored for use during time- stepping.

The FDTD electric field update equations may be simplified further for perfectly conducting materials or free space. In equation 15 if σ becomes zero (for free space), the E_x update equation becomes:

$$E_x|_{i,j,k}^{n+1} = E_x|_{i,j,k}^n + \frac{\Delta t}{\Delta y \epsilon_{i,j,k}} (H_z|_{i,j+1/2,k}^{n+1/2} - H_z|_{i,j-1/2,k}^{n+1/2}) - \frac{\Delta t}{\Delta z \mu_{i,j,k}} (H_y|_{i,j,k+1/2}^{n+1/2} - H_y|_{i,j,k-1/2}^n) \dots \dots (17)$$

This speeds computation, as fewer floating-point calculations are required. For a perfect conductor, σ is infinite and equation 16 becomes zero,

General FDTD algorithm

To implement the FDTD algorithm the problem space is subdivided into small (volume) cells each with an assigned conductivity, permittivity and permeability. Time is also discretised and the time step duration is determined by stability criterion known as the Courant Limit. Each cell is given initial values for its electric and magnetic field components: at each subsequent time step these are updated, taking account of the previous values and those of its neighbours(using the update equations). Source cells can be programmed with preset sinusoidal or impulse functions. The update process is repeated until a steady state is reached. In bioelectromagnetic, lossy tissue speeds up convergence (typically <10 sinusoidal cycles) compared with #D metal objects. One drawback is that the computational domain must have good absorbing boundaries otherwise waves propagating out will be reflected back, causing errors. Post processing of results occurs when time stepping is complete. This often includes near-to far-field conversion for the generation of radiation patterns.

Modelling of electromagnetic interactions with biological tissue.

Biological tissue is, for practical purposes, non-magnetic with permeability μ (Hm^{-1}) close to that of free space. Interaction between radio frequency electromagnetic waves and living systems therefore requires consideration of the influence of both external and internally induced fields. Energy exchanges may occur with either free charges or dipolar (asymmetrically charged) structures such as water. In a rapidly alternating field, free charges may be accelerated, giving rise to conduction currents and corresponding resistive losses, while dipoles suffer reorientation, producing frictional resistance caused

by the viscous biological medium. Both phenomena result in tissue temperature rise and account for the bulk absorption of RF energy by the biological body.

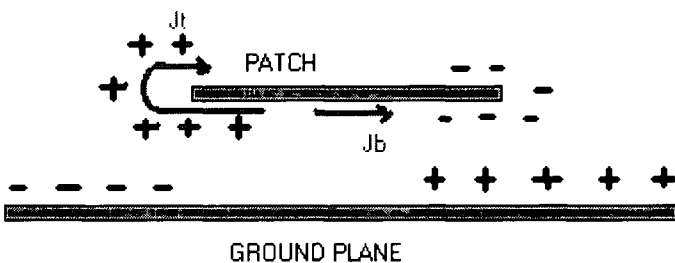
Appendix (L)

Rectangular patch using Cavity model

Microstrip antenna resemble dielectric loaded cavities, and they exhibit higher order resonance. The normalized fields within the dielectric substrate can be found more accurately by treating that region as a cavity bounded by electric conductors and by magnetic walls along the perimeter of the patch.

The cavity model consists of a box with electric walls at the upper and bottom surface and magnetic walls normal to the edges of the patch, height of it is h .

When an oscillating current is injected into a microstrip element a charge distribution is established on the surface of the ground plane and the two surfaces (upper and lower) of the patch is shown below.



Charge distribution is established on the surface of the ground plane and the two surfaces of the patch

Here are two opposing tendencies, which shape this charge distribution. There is an attractive tendency between the opposite charges at corresponding points on the lower side of the patch and on the ground plane.

Therefore it can be used to compute the field distributions inside the patch. The tangential E- field is zero at the metallic surface of the patch and the H field tangential to the wall surround the patch edge is zero. The fields of the rectangular resonator for TM_{m,n} can be expressed as follows and it is convenient to begin with the wave equation [29]

Where $kc^2 = y^2 + w^2\mu e$

The solutions of this partial differential equation is

Where $kc^2 = kx^2 + ky^2$



University of Moratuwa, Sri Lanka.
Electronic Theses & Dissertations
www.lib.mrt.ac.lk

For any TM_{mn} mode fields inside the patch

Substituting (2) in (3)

$$Ex = k_x / \omega \epsilon \mu (-C1 \sin(k_x x) + D1 \cos(k_x x)) (C2 \cos(k_y x) + D2 \sin(k_y x)) \dots \dots \dots (7)$$

Substituting (2) in (4)

$$Ey = -k_y / \omega \varepsilon \mu (C1 \cos(k_x x) + D1 \sin(k_x x)) (-C2 \sin(k_y x) + D2 \cos(k_y x)) \dots \dots \dots (8)$$

Substituting (2) in (5)

$$Hx = k_y / \mu (C1 \cos(k_x x) + D1 \sin(k_x x)) (-C2 \sin(k_y x) + D2 \cos(k_y x)) \dots \dots \dots (9)$$

Substituting (2) in (6)

$$Hy = -kx / \mu (-C1 \sin(k_x x) + D1 \cos(k_x x)) (C2 \cos(k_y x) + D2 \sin(k_y x)) \dots \quad (10)$$

The tangential E field is zero at the metallic surface of the patch, hence the boundary conditions are

Ey (0 ≤ x ≤ a, 0 ≤ y ≤ b) = 0 University of Moratuwa, Sri Lanka.....(12)
 Electronic Theses & Dissertations
www.lib.mrt.ac.lk

The tangential H field to the wall that surround the patch is zero , creating a perfect magnetic wall

Applying the above boundary conditions to the equations (7),(8),(9) and (10) and putting $a=a_1$ and $b=b_1$ because of the line extension due to the fringing fields

Where

C1 C2 = constants

The patch resonant frequency for TM mn mode is

Therefore, for TM 01 ($m=0, n=1$) (15) and (18) become

The effect of the substrate thickness University of Moratuwa, Sri Lanka.



University of Moratuwa, Sri Lanka
Electronic Theses & Dissertations
www.lib.mrt.ac.lk

The effect of the substrate thickness h , can be examined in the patch model using image theory

The field due to the image of the two z directed source is

Where $k = 2\pi / l$

For magnitude terms

For phase terms,

Substituting (19),(20),and(21) in (18) gives

Substituting (15) in (22)

$$E = -IzE_0 \cos(m\pi x/a) \cos(n\pi y/b) \cos(kh \cos(\theta)) \dots \quad (27)$$

Where



University of Moratuwa, Sri Lanka.
Electronic Theses & Dissertations
www.lib.mrt.ac.lk

Appendix (M) Calculations

(I) If frequency is 10GHz then $\lambda_0 = (2.997925 \times 10^{10} / 10^9)$ mm=29.97025 mm

$$\begin{aligned}\lambda_g &= \lambda_0 \times (\varepsilon_r)^{-1/2} \\ &= 29.97925 \times (2.91)^{-1/2} \text{ mm} \\ &= 17.5741 \text{ mm}\end{aligned}$$

$w=a = \lambda_g$ the input impedance can be calculated as following.

Length of the patch (a)=17.5741mm

Width of the patch (b) = $\lambda_g \times 0.451$

$$= 7.9259\text{mm}$$

The effective dielectric constant due to the length a

$$\epsilon_{e,a} = 2.6459$$

The effective dielectric constant due to the length b

$$\epsilon_{e,b} = 2.5047$$

The fringing field length due to the width a

$$\Delta a = 0.744 \text{ mm}$$

The fringing field length due to the width b

$$\Delta b = 0.775 \text{ mm}$$

Therefore the effective patch dimensions are,

$$a' = a + \Delta a = 18.3181 \text{ mm}$$

$$b' = b + \Delta b = 8.7009 \text{ mm}$$

The patch resonance frequency for TM01 mode



$$f_r = 10.0987 \text{ GHz}$$

(II)

If frequency is 9.4GHz then $\lambda_0 = (2.997925 \times 10^{10} / 9.4 \times 10^8) \text{ mm} = 31.8928 \text{ mm}$

$$\begin{aligned}\lambda_g &= \lambda_0 \times (\epsilon_r)^{-1/2} \\ &= 31.8928 \times (2.91)^{-1/2} \text{ mm} \\ &= 18.6957 \text{ mm}\end{aligned}$$

w=a = λ_g the input impedance can be calculated as following.

Length of the patch (a)= 18.6957 mm

$$\begin{aligned}\text{Width of the patch (b)} &= \lambda_g \times 0.451 \\ &= 8.4318 \text{ mm}\end{aligned}$$

The effective dielectric constant due to the length a

$$\epsilon_{e,a} = 2.4825$$

The effective dielectric constant due to the length b
 $\epsilon_{e,b} = 2.6258$

The fringing field length due to the width a

$$\Delta a = 0.7499 \text{ mm}$$

The fringing field length due to the width b

$$\Delta b = 0.7786 \text{ mm}$$

Therefore the effective patch dimensions are,

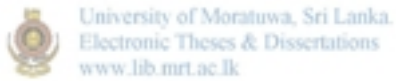
$$a' = a + \Delta a = 19.4456 \text{ mm}$$

$$b' = b + \Delta b = 9.2104 \text{ mm}$$

The patch resonance frequency for TM01 mode

$$f_r = 9.5403 \text{ GHz}$$

By using (13)



$$Y_{in} = \frac{w}{60\lambda_0}$$

$$= \frac{\lambda_g}{60\lambda_0}$$

$$Z_{in} = \frac{1}{Y_{in}} = \frac{60\lambda_0}{\lambda_g}$$

(I)

$$Z_{in} = 102.3524 \text{ ohm}$$

(II)

$$Z_{in} = 102.3523 \text{ ohm}$$

(I)

If Z_{in} is given by (15) and Z_f equals to 50 ohm, Z_t is computed as

Using figure 8,

Then the width of the transformer is = 1.9600mm

Length of the $\lambda/4$ transformer = 4.394 mm

Width of the 50 ohm line for single patch antenna = 4.16mm

When $Z_{in} = 25 \text{ ohm}$ $Z_f = 50 \text{ ohm}$

Therefore by (14)

$$Z_t = 35.35 \text{ ohm...}$$

The impedance of the 2nd and 3rd quarter wave matching transformer = 35.35 ohm

The width of the 2nd and 3rd quarter wave matching transformer = 6.125mm

(II) If Z_{in} is given by (15) and Z_f equals to 100 ohm, Z_t is computed as

Zt = $\sqrt{100 \times 102.3523} = 101.1693$ ohm

Using figure 14,

Then the width of the transformer is = 1mm

Width of the 50 ohm line for single patch antenna = 4.16mm

(II) (i) [14]

$$\phi = \frac{2\pi}{\lambda} d \sin \theta + \pi, \quad d = \lambda/2$$

(ii)

$$\phi = \frac{2\pi}{\lambda} d \sin \theta + \pi, \quad d = \lambda$$

(iii)

$$\phi = \frac{2\pi}{\lambda} d \sin \theta + \pi, \quad d = \lambda$$

(iv)

$$\phi = \frac{2\pi}{\lambda} d \sin \theta + 0, \quad d = \lambda$$

The theoretical and practical far field radiation patterns are on page 68

Appendix (N)

fdtd6()-calculation of EM radiation absorb by the human

brain using FDTD

```
function hfdfd2(nn)
nccell=2*(nn^3);
h=0.1/real(nn);
nn2=nn*2;
sig=1.29;
raw=1050.;
f=0.9e9;
w=2*pi*f;
eps0=(1e-9)/(36*pi);
eps=50.11*eps0;
u=4*pi*1e-7;
cl=3e8;
rb=1/2*u*cl;
delta=1e-2;
dt=delta/2*cl;
ra=((dt^2)/(u*eps0*delta^2));
r=dt/eps0;
ca=1-r*sig/eps;
cb=ra/eps;
cbmrb=cb/rb;

for n=1:nccell
    tau(n)=sig+i*w*(eps-eps0);
end
for ics=1:6
    if ics==1
        e0=87;
    else
        e0=100+(ics-2)*100;
    end
    ve0(ics)=e0;
    for n=1:nn2
        sax(n)=0.;
        say(n)=0.;
```



```

saz(n)=0.;
htx(n)=0.;
hty(n)=0.;
htz(n)=0.;
end

n=0;
spow=0.;
shta=0.;

Ex(1)=1;
Ey(1)=1;
Ez(1)=1;
Hx(1)=1;
Hy(1)=1;
Hz(1)=1;

for t=2:10
    for jj=1:nn
        for ii=1:nn2
            for kk=1:nn
                Hx(t)=Hx(t-1)+rb*(Ey(t-1)+Ez(t-1));
                Hy(t)=Hy(t-1)+rb*(Ez(t-1)+Ex(t-1));
                Ex(t)=ca*Ex(t-1)+cbmrb*(Hz(t-1)-Hy(t-1));
                Ey(t)=ca*Ey(t-1)+cbmrb*(Hx(t-1)-Hz(t-1));anka
                Ez(t)=ca*Ez(t-1)+cbmrb*(Hy(t)-Hx(t));secretations
                Hz(t)=Hz(t-1)+rb*( Ex(t-1)-Ey(t-1));

                n=n+1;
                pow=((abs(Ex(t)))^2+(abs(Ey(t)))^2+(abs(Ez(t)))^2);
                sa=0.5*pow*(sig/raw);
                sar=sar;
                hta(n)=0.5*sig*pow*1.e-3;
                ssar(ii,jj,kk)=sa;
                spow=spow+sa;
                shta=shta+hta(n);
                sax(ii)=sax(ii)+sa;
                say(jj+nn)=say(jj+nn)+sa;
                j1=nn-jj+1;
                say(j1)=say(j1)+sa;
                saz(kk+nn)=saz(kk+nn)+sa;
                k1=nn-kk+1;
                saz(k1)=saz(k1)+sa;
            end
        end
    end
e0
sar
max(sar,[],2)
mean(sar,2)

```

```

hta
max(hta,[],2)
mean(hta,2)
end
sam=-0.000001;
for ii=1:nn2
    cd(ii)=real(ii)*h;
    if sax(ii) > sam
        sam=sax(ii);
    end
    if say(ii) > sam
        sam=say(ii);
    end
    if saz(ii) > sam
        sam=saz(ii);
    end
end
for ii=1:nn2
    sax(ii)=sax(ii)/sam;
    say(ii)=say(ii)/sam;
    saz(ii)=saz(ii)/sam;
end
plot(cd,sax,cd,say,cd,saz,cd,sax,'r','cd',say,'r+','cd',saz,'r*')
title('Relative Energy Absorbed ')
text(.025,.95,'Frequency 900 Mhz.')
text(.025,.90,'No. cells 1000 ')
text(.025,.85,'Fl. Int. V/m')
xlabel('x- X axis, + Y - axis, * Z - axis (m.)')
ylabel('Relative Energy Absorbed')
input z
power(ics)=spow/nccell;
tht(ics)=shta;
r(ics)=power(ics)/tht(ics);
end
ve0
power
tht
r
input zz;
plot(ve0,power,'r-',ve0,power,'r+')
title('Graph of Energy Absorbed vs. Field Intensity')
text(55.,19.,'Frequency 900 Mhz.')
text(55.,17.,'No cells 1000')
xlabel('Field Intensity (V/m)')
ylabel('Energy Absorbed (mW/gm.)')

```

Appendix (O)

fdtd7()-calculation of EM radiation absorb by the human brain and skull using FDTD

```
*****
function hfdd3(nn)
ncell=2*(nn^3);
h=0.1/real(nn);
nn2=nn*2;
sig=1.29;
raw=1050.;
f=0.9e9;
w=2*pi*f;
eps0=(1e-9)/(36*pi);
eps=50.11*eps0;
u=4*pi*1e-7;
cl=3e8;
rb=1/2*u*cl;
delta=1e-2;
dt=delta/2*cl;
ra=((dt^2)/(u*eps0*delta^2));
r=dt/eps0;
ca=1-r*sig/eps;
cb=ra/eps;
cbmr=cb/rb;

for ii=1:nn2
    for jj=1:nn
        for kk=1:nn
            n=n+1;
            if (ii>1 | ii<nn2) & (jj<nn) & (kk<nn)
                tau(n)=sig+i*w*(eps-eps0);
            else
                tau(n)=sig1*i*w*(eps-eps0);
            end
        end
    end
end
for ics=1:6
    if ics==1
        e0=87;
    else
        e0=100+(ics-2)*100;
```



```

end
ve0(ics)=e0;
for n=1:nn2
    sax(n)=0.;
    say(n)=0.;
    saz(n)=0.;
    htx(n)=0.;
    hty(n)=0.;
    htz(n)=0.;
    end
n=0;
spow=0.;
shta=0.;
Ex(1)=1;
Ey(1)=1;
Ez(1)=1;
Hx(1)=1;
Hy(1)=1;
Hz(1)=1;
for t=2:10
    Hx(t)=Hx(t-1)+rb*(Ey(t-1)+Ez(t-1));
    Hy(t)=Hy(t-1)+rb*(Ez(t-1)+Ex(t-1));
    Ez(t)=ca*Ex(t-1)+cbmrb*(Hz(t-1)-Hy(t-1));
    Ey(t)=ca*Ey(t-1)+cbmrb*(Hx(t-1)-Hz(t-1));
    Ez(t)=ca*Ez(t-1)+cbmrb*(Hy(t)-Hx(t));
    Hz(t)=Hz(t-1)+rb*( Ex(t-1)-Ey(t-1));
    n=n+1;
    pow=((abs(Ex(t)))^2+(abs(Ey(t)))^2+(abs(Ez(t)))^2);
for jj=1:nn
    for ii=1:nn2
        for kk=1:nn
            n=n+1;
            pow=(abs(e(n)))^2+(abs(e(n+ncell)))^2+(abs(e(n+2*ncell)));
            if (ii>1 | ii<nn2) & (jj<nn) & (kk<nn)
                sa=(sig/raw)*pow;
                sar(n)=sa;
                hta(n)=.5*sig*pow*1.e-3;
            else
                sa=(sig1/raw1)*pow;
                sar(n)=sa;
                hta(n)=.5*sig1*pow*1.e-3;
            end
            if (ii>1 | ii<nn2) & (jj<nn) & (kk>-nn | kk<-nn2)
                sa=(sig2/raw2)*pow;
                sar(n)=sa;

```

```

hta(n)=0.5*sig2*pow*1.e-3;
end
ssar(ii,jj,kk)=sa;
spow=spow+sa;
shta=shta+hta(n);
sax(ii)=sax(ii)+sa;
say(jj+nn)=say(jj+nn)+sa;
j1=nn-jj+1;
say(j1)=say(j1)+sa;
saz(kk+nn)=saz(kk+nn)+sa;
k1=nn-kk+1;
saz(k1)=saz(k1)+sa;
end
end
end
e0
sar
max(sar,[],2)
mean(sar,2)
hta
max(hta,[],2)
mean(hta,2)
end
sam=-0.000001;
for ii=1:nn2
cd(ii)=real(ii)*h;
if sax(ii) > sam
    sam=sax(ii);
end
if say(ii) > sam
    sam=say(ii);
end
if saz(ii) > sam
    sam=saz(ii);
end
end
for ii=1:nn2
sax(ii)=sax(ii)/sam;
say(ii)=say(ii)/sam;
saz(ii)=saz(ii)/sam;
end
plot(cd,sax,cd,say,cd,saz,cd,sax,'rx',cd,say,'r+',cd,saz,'r*')
title('Relative Energy Absorbed ')
text(.025,.95,'Frequency 900 Mhz.')
text(.025,.90,'No. cells 1000 ')

```



```

text(.025,.85,'Fld. Int.    V/m')
xlabel('x- X axis, + Y - axis, * Z - axis (m.)')
ylabel('Relative Energy Absorbed')
input z
power(ics)=spow/ncell;
tht(ics)=shta;
r(ics)=power(ics)/tht(ics);
end
ve0
power
tht
r
input zz;
plot(ve0,power,'r-',ve0,power,'r+')
title('Graph of Energy Absorbed vs. Field Intensity')
text(55.,19.,'Frequency 900 Mhz.')
text(55.,17.,'No cells 1000')
xlabel('Field Intensity (V/m)')
ylabel('Energy Absorbed (mW/gm.)')

```

Appendix (P)



University of Moratuwa, Sri Lanka.
Electronic Theses & Dissertations
<http://www.mech.uom.ac.lk>

fDTD8()-calculation of EM radiation absorb by the human

brain, skull and ear using FDTD

```

*****
function hfdtd4(nn)
ncell=2*(nn^3);
h=0.1/real(nn);
nn2=nn*2;
sig=1.29;
raw=1050.;
f=0.9e9;
w=2*pi*f;
eps0=(1e-9)/(36*pi);
eps=50.11*eps0;
u=4*pi*1e-7;
cl=3e8;
rb=1/2*u*cl;
delta=1e-2;
dt=delta/2*cl;
ra=((dt^2)/(u*eps0*delta^2));
r=dt/eps0;

```

```

ca=1-r*sig/eps;
cb=ra/eps;
cbmrbc=cb/rb;

n=0;
for ii=1:nn2
    for jj=1:nn
        for kk=1:nn
            n=n+1;
            if (ii>1 | ii<nn2) & (jj<nn) & (kk<nn)
                tau(n)=sig+i*w*(eps-eps0);
            else
                tau(n)=sig1*i*w*(eps-eps0);
            end
            if (ii==1 & ii==nn*2) & (jj==nn) & (kk==0)
                tau(n)=sig+i*w*(eps-eps0);
            end;
        end
    end
end
for ics=1:6
    if ics==1
        e0=87;
    else
        e0=100+(ics-2)*100;
    end
    ve0(ics)=e0;
    for n=1:nn2
        sax(n)=0.;
        say(n)=0.;
        saz(n)=0.;
        htx(n)=0.;
        hty(n)=0.;
        htz(n)=0.;
    end
    n=0;
    spow=0.;
    shta=0.;
    Ex(1)=1;
    Ey(1)=1;
    Ez(1)=1;
    Hx(1)=1;
    Hy(1)=1;
    Hz(1)=1;
    for t=0.2:1
        Hx(t)=Hx(t-1)+rb*(Ey(t-1)+Ez(t-1));

```



```

Hy(t)=Hy(t-1)+rb*(Ez(t-1)+Ex(t-1));
Ex(t)=ca*Ex(t-1)+cbmrb*(Hz(t-1)-Hy(t-1));
Ey(t)=ca*Ey(t-1)+cbmrb*(Hx(t-1)-Hz(t-1));
Ez(t)=ca*Ez(t-1)+cbmrb*(Hy(t)-Hx(t));
Hz(t)=Hz(t-1)+rb*( Ex(t-1)-Ey(t-1));
n=n+1;
for jj=1:nn
    for ii=1:nn2
        for kk=1:nn
            n=n+1;
            pow=(abs(e(n)))^2+(abs(e(n+ncell)))^2+(abs(e(n+2*ncell)));
            if (ii>1 | ii<nn2) & (jj<nn) & (kk<nn)
                sa=(sig/raw)*pow;
                sar(n)=sa;
                hta(n)=.5*sig*pow*1.e-3;

            else
                sa=(sig1/raw1)*pow;
                sar(n)=sa;
                hta(n)=.5*sig1*pow*1.e-3;
            end
            if (ii==1 & ii==nn*2) & (jj==nn) & (kk==0)
                sa=(sig/raw)*pow;
                sar(n)=sa;
                hta(n)=.5*sig*pow*1.e-3;
            end;
            ssar(ii,jj,kk)=sa;
            spow=spow+sa;
            shta=shta+hta(n);
            sax(ii)=sax(ii)+sa;
            say(jj+nn)=say(jj+nn)+sa;
            j1=nn-jj+1;
            say(j1)=say(j1)+sa;
            saz(kk+nn)=saz(kk+nn)+sa;
            k1=nn-kk+1;
            saz(k1)=saz(k1)+sa;
            end
        end
    end
end
e0
sar
max(sar,[],2)
mean(sar,2)
hta

```

```

max(hta,[],2)
mean(hta,2)
end
sam=-0.000001;
for ii=1:nn2
    cd(ii)=real(ii)*h;
    if sax(ii) > sam
        sam=sax(ii);
    end
    if say(ii) > sam
        sam=say(ii);
    end
    if saz(ii) > sam
        sam=saz(ii);
    end
end
for ii=1:nn2
    sax(ii)=sax(ii)/sam;
    say(ii)=say(ii)/sam;
    saz(ii)=saz(ii)/sam;
end
plot(cd,sax,cd,say,cd,saz,cd,sax,'rx',cd,say,'r+',cd,saz,'r*')
title('Relative Energy Absorbed ')
text(.025,.95,'Frequency 900 Mhz.')
text(.025,.90,'No. cells 1000 ')
text(.025,.85,'Fld. Int. V/m')
xlabel('x- X axis, + Y - axis, * Z - axis (m.)')
ylabel('Relative Energy Absorbed')
input z
power(ics)=spow/nccell;
tht(ics)=shta;
r(ics)=power(ics)/tht(ics);
end
ve0
power
tht
r
input zz;
plot(ve0,power,'r-',ve0,power,'r+')
title('Graph of Energy Absorbed vs. Field Intensity')
text(55.,19.,'Frequency 900 Mhz.')
text(55.,17.,'No cells 1000')
xlabel('Field Intensity (V/m)')
ylabel('Energy Absorbed (mW/gm.)')

```

Appendix (Q)

prog() - Dimensions of the patches

```
function prog()
f=input('DESIGN FREQUENCY IN GHz      ');
u1=0.29979/f;
uu=u1*1000;
h=1.6;
ee=sqrt(2.91);
u=uu/ee;
a=u;
b=u*0.451;
DESIGN_FREQUENCY _____ GHz = f
WIDTH_OF_THE_PATCH_____mm = a
LENGTH_OF_THE_PATCH_____mm = b
E=2.91;
Ea=((E+1)/2)+((E-1)/2)*(1/sqrt(1+(10*h/b)));
Eb=((E+1)/2)+((E-1)/2)*(1/sqrt(1+(10*h/a)));
La=0.412*h*((Ea+0.3)/(Ea-0.258))*(((b/h)+0.262)/ ((b/h)+0.813));
Lb=0.412*h*((Eb+0.3)/(Eb-0.258))*(((a/h)+0.262)/ ((a/h)+0.813));
a1=a+La;
b1=b+Lb;
bb=(b1)/1000;
fr=((299.79e6)/(2*bb*ee))/1e9;
RESONANCE_FREQUENCY _____ GHz = fr
z=60*uu/a1;
INPUT_IMPEDANCE_OF_THE_PATCH____ohms = z
Zt=sqrt(50*z);
IMPEDANCE_OF_THE_QUATER_WAVE_TRANSFORMER_ohms = Zt
W_h_RATIO=input('ENTER THE W/H RATIO      ')
WI=W_h_RATIO*1.6;
WIDTH_QUATER_WAVE_TRANSF_mm = WI
IN=2.588235*1.6;
WDTH_50_TRANSMISSION_LINE_mm = IN
```

Appendix(R)

```
*****
```

impedance()-graph of the impedance

```
*****
```

```
function antennal()
z=102.9
e=2.91
%a=.1
t=0.01;
wq=0;
for a= 0.05:.1:9,
wq=wq+1;
A=a;
t=t+0.01;
w=a*1.5;
SS(1,wq) = (377/sqrt(e))/((a)+0.8825+0.1645*((e-1)/e*e) +
((e+1)/(pi*e))*(1.451+log((a/2)+0.94)));  
of Moratuwa, Sri Lanka.  
Electronic Theses & Dissertations  
www.lib.mrt.ac.lk
end
plot(SS)
axis([0 90 0 120])
grid on
xlabel(' w/h ratio ')
ylabel( 'Impedance ohms ')
title('Graph of impedance of a microstrip transmission line')
```

Appendix (S)

```
*****
```

array2()- Theoretical radiation patterns

```
*****
```

```
function array2()
lam0=29.979;
lam=17.5741;
d=2*lam;
n=1;
k0=(2*pi)/lam0;
k=(2*pi)/lam;
h=1.6;
b1=8.7;
b2=0.775;
for ii=54:90
    theta(ii)=(5*ii)*pi/180;
    f(ii)=(2*pi/lam)*d*cos(theta(ii));
    f2(ii)=(1/n)*((sin(n*f(ii)/2))/sin(f(ii)/2));
    f3(ii)=(cos((k*h)*(cos(theta(ii)))))*((sin(k0*(b2/2)*(sin(theta(ii)))))./
    (k0*(b2/2)*(sin(theta(ii)))))*(cos(k0*(b1/2)*(sin(theta(ii)))));
    f5(ii)=abs(f2(ii)*f3(ii));
end
theta;
f5;
polar(theta,f5)
```



Appendix (T)

```
*****
```

Array3()- theoretical radiation patterns

```
*****
```

```
function array3()
lam0= 31.8928;
lam= 18.6957;
d=lam/2;
n=2;
k0=(2*pi)/lam0;
k=(2*pi)/lam;
h=1.6;
b1= 9.2104;
b2= 0.7786;
for ii=54:90
    theta(ii)=(5*ii)*pi/180;
    f(ii)=((2*pi/lam)*d*cos(theta(ii))+pi);
    f2(ii)=(1/n)*((sin(n*f(ii)/2))/sin(f(ii)/2));
    f3(ii)=(cos((k*h)*(cos(theta(ii))))*((sin(k0*(b2/2)*(sin(theta(ii)))))/(k0*(b2/2)*(sin(theta(ii)))))*(cos(k0*(b1/2)*(sin(theta(ii))))));
    f5(ii)=abs(f2(ii)*f3(ii));
end
theta;
f5;
polar(theta,f5)
```

Appendix (U)

August 6th

'MOBILE PHONE GAVE ME CANCER' SAYS DOCTOR

An American doctor suffering from terminal cancer is suing mobile phone companies for £600 million.

Dr Chris Newman (pictured) claims his brain tumour is a direct result of electromagnet radiation from his mobile phone.

In a major testcase with worldwide implications, he is suing mobile phone manufacturers and network operators for damages. "Never use a cell phone – it's not worth the risk; it's not worth going through the hell," he said.

'No evidence'

US health authorities say there is no evidence to prove or disprove any link between mobile phone use and brain tumours.

In the UK, the Government has urged parents and teachers to discourage children from using mobile phones because of the safety fears.

There is also a strong push, in the UK and in the US, for health warnings to be placed on mobile phones.

New UK study

And a new safety study into mobile phones has been launched in the UK following fresh evidence about hands-free kits from Australian researchers.

The Australian evidence suggests hands-free kits can cut radiation levels by 92 per cent, conflicting with an earlier study indicating that hands-free kits could actually triple the amount of radiation to the brain.

The UK Consumers Association has commissioned further research "to clear up the confusion" in light of the Australian Consumers' Association investigation.



University of Moratuwa, Sri Lanka.
Electronic Theses & Dissertations
www.lib.mrt.ac.lk

Send us your comments
© 2000 sky.com

Appendix (V)

Cellular system used in Sri Lanka

Company	System	Frequency
Call Link	TACS A	890-915 m-b 935-960 b-m
Celltel	TACS B	872-888 m-b 917-933 b-m
Mobitel	AMPS A/AMPS B	825-845 m-b 870-890 b-m
Dialog	GSM	890-915 m-b 935-960 b-m

Power of Mobile Phone for AMPS

Power Level	Power of Mobile Phone for AMPS						
	Mobile Station Power Class						
	I		II		III		
	dBW	mW	dBW	mW	dBW	mW	
0	6	4000	2	1600	2	630	
1	2	1600	2	1600	2	630	
2	-2	630	-2	630	-2	630	
3	-6	250	-6	250	-6	250	
4	-10	100	-10	100	-10	100	
5	-14	40	-14	40	-14	40	
6	-19	15	-18	15	-18	15	
7	-22	6	-22	6	-22	6	

Power of Mobile Phone for TACS

Power Level	Power of Mobile Phone for TACS								
	Mobile Station Power Class								
	I		II		III		IV		
	dBW	mW	dBW	mW	dBW	mW	dBW	mW	
0	10	10000	6	4000	2	1600	2	630	
1	2	1600	2	1600	2	1600	2	630	
2	-2	630	-2	630	-2	630	-2	630	
3	-6	250	-6	250	-6	250	-6	250	
4	-10	100	-10	100	-10	100	-10	100	
5	-14	40	-14	40	-14	40	-14	40	
6	-19	15	-18	15	-18	15	-18	15	
7	-22	6	-22	6	-22	6	-22	6	



University of Moratuwa, Sri Lanka
 Electronic Theses & Dissertations
www.lib.mrt.ac.lk

